Sensors and Actuators B 242 (2017) 912–920

Contents lists available at ScienceDirect

Sensors and Actuators B: Chemical

journal homepage: www.elsevier.com/locate/snb

Simultaneous measurement of refractive index and temperature using a SPR-based fiber optic sensor

Jesús Salvador Velázquez-González[a,b], David Monzón-Hernández[a,*], David Moreno-Hernández[a], Fernando Martínez-Piñón[b], Iván Hernández-Romano[c]

[a] Centro de Investigaciones en Óptica A. C., Loma del Bosque 115, C.P. 37150, León, Gto., México
[b] Instituto Politécnico Nacional (IPN) – Centro de Investigación e Innovación Tecnológica (CIITEC), Cerrada de Cecati S/N. Col. Santa Catarina, Azcapotzalco, Ciudad de México, C.P. 02250, México
[c] CONACYT-Electronics Department, Sede Palo Blanco, University of Guanajuato, Carr. Salamanca-Valle de Santiago Km 3.5+1.8, Salamanca, Guanajuato C.P. 36885, México

ARTICLE INFO

Article history:
Received 7 June 2016
Received in revised form
23 September 2016
Accepted 27 September 2016
Available online 28 September 2016

Keywords:
Refractive index and temperature sensing
Optical fiber sensors
Metal deposition
Surface plasmon resonance
Polydimethylsiloxane (PDMS)

ABSTRACT

A surface plasmon resonance-based fiber-optic sensor for simultaneous measurement of refractive index and temperature of liquid samples is proposed and experimentally demonstrated. The sensor consists of a gold-coated MM-SM-MM optical fiber structure, whose sensitive section was partially covered with polydimethylsiloxane (PDMS) to generate two independent SPR resonance dips in the fiber transmission spectrum. One of the dips is generated by the bare gold-coated fiber section whose wavelength resonance is tuned by the refractive index and temperature of the surrounding medium. The other dip that is exclusively used to monitor the temperature variations of the liquid sample, whose central wavelength at 900 nm corresponds to PDMS refractive index at 20 °C, is produced by the polymerized gold-coated fiber section. The high refractive index and temperature sensitivity achieved, 2323.4 nm/RIU and −2.850 nm/°C respectively, the small size, the ease fabrication process, and the bio-compatibility of the proposed device are appealing characteristics that makes it ideal for practical bio-sensing applications.

1. Introduction

Optical fiber refractive index sensors (OFRIS) have been extensively studied during the last four decades. Owing to the intrinsic characteristics of the optical fiber, these sensors are in general simple to fabricate, compact, robust, immune to electromagnetic radiation, chemical and biological inert, and can be integrated in complex networks for real-time multiparameter sensing. In recent years the important advances achieved in the fiber optic sensing technology; in terms of sensitivity, resolution, dynamic range, response time, signal to noise ratio and fabrication techniques, have promoted the development of optical fiber chemical sensors and biosensors [1–6]. On the other hand, it is well known that performance of high-resolution OFRIS is greatly affected by environmental temperature perturbations due to the strong influence of temperature in the refractive index. To reduce the refractive index measurement uncertainty due to temperature perturbation, the common approach involves the simultaneous measurement of both parameters. In the simplest scheme the sensing head is composed by a pair of cascaded [7–15] or embedded [16–21] optical fiber devices, with good sensitivity to these two parameters. The performance is quite similar, but the former approach is not suitable to fabricate compact sensors since the total length of the devices is around tens of millimeters. Sensors in which devices are superimposed or embedded are compact but the fabrication process is in general complicated and requires specialized equipment. In an ideal scenario, each device should respond to exclusively one single parameter, however, in practice this rarely occurs. In practically all the methods proposed so far, at least one of the devices is sensitive to refractive index as well as temperature.

OFRIS based on surface plasmon resonance phenomenon offers a unique platform for development of modern biosensors due to the ultra-high sensitivity and resolution capabilities exhibited, the fast response and the possibility for real time detection [22–27]. Conventional single-signal SPR-based fiber-optic sensors are unable to compensate the effects of environmental perturbations. External temperature fluctuations generate a significant change in the SPR signal that could lead to incorrect refractive index measurements.

* Author to whom correspondence should be addressed.
E-mail address: dmonzon@cio.mx (D. Monzón-Hernández).

http://dx.doi.org/10.1016/j.snb.2016.09.164
0925-4005/

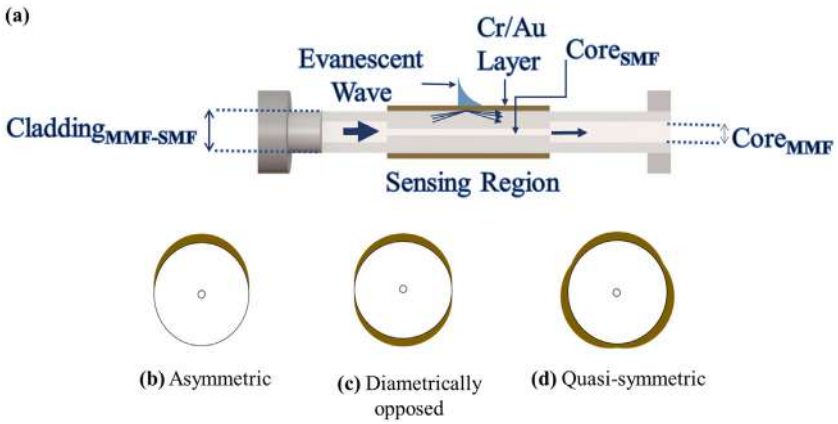

Fig. 1. (a) MM-SM-MM structured fiber composed by a single mode fiber section of length L inserted into a multimode fiber. Cross-section of a fiber fabricated and the geometry of the gold thin film deposited over the fiber with (b) single, (c) two and (d) three evaporations.

In order to isolate the SPR fiber optic refractive index sensor from external perturbations a common scheme, successfully exploited in prism-based SPR sensors [28,29], consists on the use of two independent metal coated fiber sections in series, one of them covered with a dielectric layer acts as a reference, to produce a double-channel SPR [30–32]. Other interesting structures, for example, a SPR refractive index sensor in cascade with a Fabry-Perot interferometer for temperature sensing has been proposed to demonstrate that it is possible to reduce the external temperature perturbation effects on the response of a SPR biosensor [33]. However, there are two aspects that could seriously limit the exploitation of these proposals; the first is relating with the fact that the outer diameter of the employed optical fiber is larger than the fiber used in standard communication networks, and the second is regarding the total length of the sensor, which is too long (several centimeters). Recently, a novel SPR sensor for simultaneous sensing of temperature and refractive index based on standard SMF with two orthogonal polished section covered with gold and silver, was proposed and demonstrated [34]. This device is compact but the fabrication process is complicated.

The high sensitivity of OFRIS based on SPR made them especially vulnerable to the undesirable effects of temperature fluctuations, the simultaneous measurement of these two parameters is a feasible alternative to face this problem. Here, we propose and demonstrate a simple-to-construct and highly sensitive dual-channel SPR-based fiber optic sensor for simultaneous measurement of refractive index and temperature. The sensor consists of MM-SM-MM structured fiber formed when a single-mode fiber (SMF) section of length L is inserted between two multimode fibers (MMF). Due to the core diameter mismatch, part of the light coupled to the SMF propagates as cladding modes where the evanescent wave interacts with external medium. The SMF section was coated with a 5 nm thin film of chromium to facilitate the adherence of a 30 nm thin film of gold. In order to generate a dual SPR signal in the same gold-coated fiber section, half length of the gold-coated SMF was covered with PDMS, which has a high negative thermo-optic coefficient (TOC). After curing, a single resonance dip around 920 nm appeared in the transmission spectrum. When fiber sensor is immersed in water-glycerol solutions another peak in the wavelength range from 600 to 750 nm appeared. The optical fiber sensor was immersed in these solutions and then the temperature was increased from 20 to 60 °C. The resonance dip produced by the bare gold-coated fiber section exhibited a sensitivity of 2323.4 nm/RIU and −280 pm/°C to refractive index and temperature, respectively. While the resonance dip of the polymer-covered fiber section only exhibited a measurable displacement when temperature changes, with a sensitivity of −2.850 nm/°C. The characteristic equation to determine the refractive index and temperature changes by analyzing the resonance dips displacements is also described.

2. SPR-based optical fiber sensor: fabrication and characterization

The multimode-single-mode-multimode (MM-SM-MM) optical fiber structure used in this study is represented in Fig. 1(a), it consists of two graded-index multimode fibers (62.5/125 μm) spliced to the ends of a conventional step-index single-mode fiber (9/125 μm) piece of length L. The process to fabricate the structure is simple since it is accomplished following the well-stablished optical fiber splicing procedure; moreover, it only takes few minutes. The rigorous analysis of the MM-SM-MM structure is an arduous problem, out of the scope of this work, discussed in detail somewhere else [35,36]. But the working mechanism can be briefly described as follows: in this structured waveguide the local discontinuity will lead to coupling mode phenomenon between incident and transmitted modes at each splice [36]. Core modes of the lead-in multimode fiber will couple to core and cladding modes at the single-mode fiber section. Cladding modes interact with the external medium through the evanescent field, which induce a significant light transmission loss when external refractive index approach to that of the cladding [37]. However, its sensitivity is virtually null to refractive indexes of biological interest, close to that of the water [37]. Coating the sensitive section of MM-SM-MM fiber with a gold thin film, in order to generate surface plasmon resonance, is a simple and viable alternative to enhance the evanescent wave interaction with external medium and this increases the RI sensitivity of the fiber. Experimental demonstration of SPR in MM-SM-MM fiber coated with gold and silver has been demonstrated [38,39]. Although gold adherence to silica fiber is poorer than silver, it is more resistant to organic solvents traditionally used to clean and remove residues adhered to the fiber during refractive index measurements. The adherence issue was traditionally solved by using a bond intermediate material, like chromium [40,41], but other methods like increasing the optical fiber surface roughness by chemical vapor etching [42], or silanizing the surface of the optical fiber by chemical process [25], have demonstrated to be a good alternative. Cylindrical geometry of the fiber imposes some challenges regarding the fiber coating process. In order to obtain a uniform layer thickness around the whole circumference of the fiber, some authors have proposed to introduce a rotatory system into the evaporation chamber [5,44–46]. In addition, since SPR is a polarization-dependent phenomenon [40–44], by depositing a homogenous symmetric layer over the perimeter of a fiber section such dependence can be eliminated [44]. However, this technique

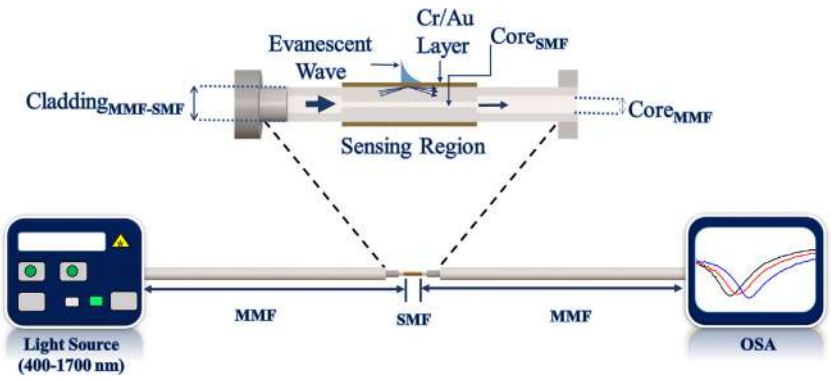

Fig. 2. Schematic representation of the set-up used to characterize samples.

increases the complexity, time, duration and costs of the fabrication process, since every fiber needs to be coated individually. In order to simplify this stage, MM-SM-MM fibers were coated following three different, though simple and stationary, procedures to yield three metal layer geometries, which are represented in Fig. 1, (b) an asymmetric [47,48], (c) two diametrically opposed [44], and (d) quasi-symmetric gold layer [49]. These three structures depend on polarization but its influence decreases as the number of layers increase since much extension of the fiber perimeter is covered [44]. In reference [50] is described the coating procedure that we followed to obtain these kind of non-symmetric geometries, the procedure allow us to fabricate several samples simultaneously with good reproducibility. The effect of the no-symmetric gold layer, deposited around the SMF section, along with the effect of SMF sensing length in the SPR signal are analyzed.

MM-SM-MM fibers samples with SMF lengths of 1, 5 and 10 mm were fabricated and then coated with a 5 nm layer of chromium followed by a 30 nm layer of gold using a conventional thermal evaporation process. Gold pellets of 99.9% purity were used. After coating, the response of the gold-coated MM-SM-MM structured fibers to external refractive index changes were characterized by measuring the spectral shift of the SPR wavelength resonance dip. The experimental set-up used is very simple and consists of a white light source and an optical spectrum analyzer, a schematic representation is shown in Fig. 2. Although, surface plasmon resonance phenomenon is strongly dependent on the polarization of electric field, this dependence can be reduced or even eliminated when the symmetry of the metal layer around the surface of the optical fiber increases [44]. In our scheme the elements to control the polarization of the light were eliminated in order to simplify the experimental set-up. The transmitted spectra, when fibers were immersed in calibrated refractive index Cargille oils (1.365-1.395 in steps of 0.005), were recorded and analyzed. The transmitted spectra of a device with SMF section of 1 mm, coated with an (a) single asymmetric layer, (b) two diametrically opposed layers and (c) quasi-symmetric gold layer, when it was immersed in oils with refractive index of 1.365 (black line), 1.375 (red line) and 1.385 (blue line) are shown in Fig. 3. These spectra were normalized to that of the air. The homogeneity of the gold layer around the fiber is improved as the number of evaporations is increased, reducing the polarization dependence [44], and this produces an enhancement of the interaction of the evanescent wave with the gold layer. As a consequence, the depth of the resonance dip increases. Although all the evaporations were the same, a red-shift in the resonance dip of the spectra is observed as the number of evaporations increases, this behavior can be explained by the fact that the gold layer thickness around the fiber augments as the number of evaporations is increased. The devices with an asymmetric layer, where a polarization control is required [41,44,47], were discarded from the rest

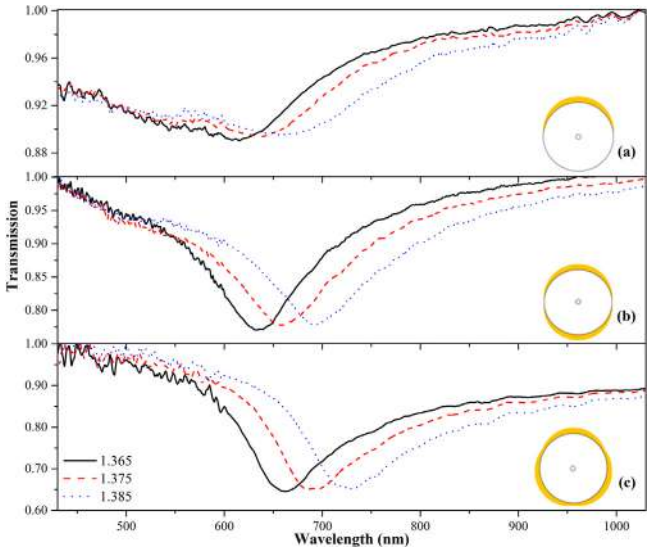

Fig. 3. Transmission spectra of the MM-SM-MM fibers with a SMF length of 1 mm and coated with an (a) asymmetric, (b) diametrically opposed and (c) quasi-symmetric gold layer. Optical fibers were immersed in Cargille oils with nominal refractive index of 1.365 (black line), 1.375 (red line) and 1.385 (blue line). (For interpretation of the references to colour in this figure legend, the reader is referred to the web version of this article.)

of the study since they exhibited the smallest dip and the highest losses. An important aspect to notice is the symmetry of the transmitted spectra of the fiber coated with a double gold layer (Fig. 3(b)) respect to the other two samples. The same symmetry is observed in the spectra of fiber samples with SMF length of (a) 1, (b) 5 and (c) 10 mm coated with a double-sided gold layer shown in Fig. 4. Since the gold layer thickness is the same for these three samples, the wavelength of the resonance dip is the same when the fibers are immersed in the same Cargille oil. The width of the dip also increases as the length of the SMF section increases. In Figs. 3 and 4, the resonance dip shifts towards longer wavelengths as the refractive index of the external medium increases. The refractive index sensitivity of the samples tested were very similar, so any of them can be used to fabricate the sensor to measure temperature and refractive index. But the fiber sample with the SMF length of 5 mm coated with a double-sided gold layer, whose dip exhibited the better shape characteristics, was selected. The calculated sensitivity of this device was around 3030 nm/RIU in the range of 1.365-1.395.

In order to quantify its temperature sensitivity, this fiber was immersed in distilled water and then heated from 20 to 60 °C. In Fig. 5 the spectral change of the SPR signal is shown. A blue-shift of the resonance dip is observed and a sensitivity of −360 pm/°C was estimated using the linear regression shown in the graph (squares)

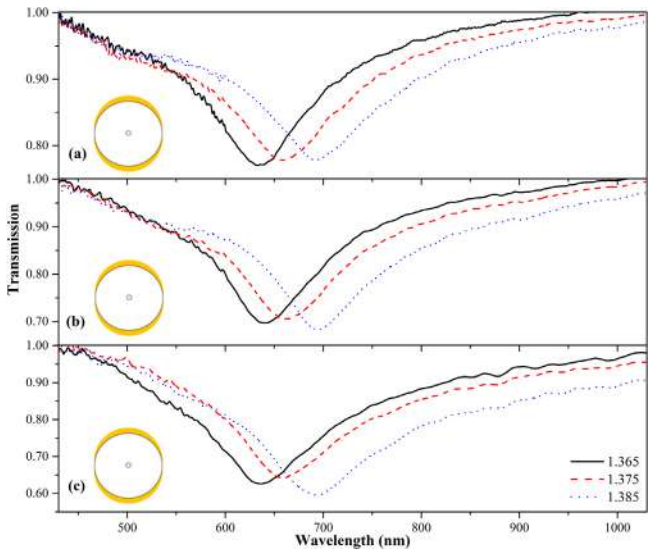

Fig. 4. Transmission spectra of the MM-SM-MM fibers coated with two diametrically opposed gold layers and with a SMF length of (a) 1, (b) 5 and (c) 10 mm. Optical fibers were immersed in Cargille oils with nominal refractive index of 1.365 (black line), 1.375 (red line) and 1.385 (blue line). (For interpretation of the references to colour in this figure legend, the reader is referred to the web version of this article.)

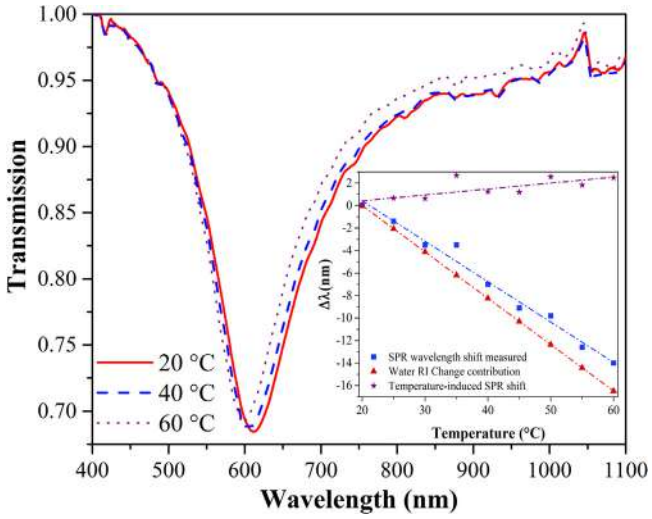

Fig. 5. Transmission spectra of the MM-SM-MM fiber with a SMF length of 5 mm and coated with a two diametrically opposed gold layers immersed in distilled water at 20 (red line), 40 (blue line) and 60 °C (purple line). In the inset is shown the SPR measured net resonance dip wavelength shifts, shift from the RI change of water and the difference between two (due to the inherit temperature sensitivity of the sensor itself). (For interpretation of the references to colour in this figure legend, the reader is referred to the web version of this article.)

of the inset of Fig. 5. This wavelength shift is mainly due to the contribution of the water refractive index change with temperature (triangles), calculated following the procedure described in ref [51]. Subtracting the refractive index change (triangles) of the water from the sensor sensitivity (squares) it is possible to estimate the intrinsic temperature sensitivity of the gold-coated fiber (stars), that has a linear fit with slope of 52 pm/°C.

3. Dual signal SPR-based optical fiber

When a SPR-based fiber optic refractive index sensor is immersed in a liquid with high TOC, for example ethanol [52], the resonance dip can be tuned by temperature. A simple temperature sensor can be achieved by covering the gold-coated fiber with PDMS whose TOC (-4.66×10^{-4}) is similar to that of ethanol. Polymer-covered fiber are easy to manipulate, a number of designs can be fabricated, but the upmost advantage is the simplicity in the fabrication process. In this regard, a step forward can be made by just covering the half-length of the gold-coated SMF section with PDMS. A representation of the proposed device is shown in Fig. 6(a) and (b), in which the half-length of the gold-coated fiber section was covered with PDMS, this section is permanently immersed in a temperature dependent refractive index ($n_{PDMS}(T)$) medium. The bare gold-coated fiber section is still sensitive to external medium refractive index changes. This is a very simple technique to create a dual-channel SPR optical fiber sensor with two independent sensing regions in the same SMF section, which can be used to measure temperature and refractive index simultaneously. The conditions and characteristics of the dual-channel SPR optical fiber sensor just described were theoretically simulated following the procedure described in [54,55]. When the device is immersed in a 90%water-10%glycerol solution with refractive index of 1.346 at 20 °C, the transmission spectra, black line in Fig. 7(a), exhibits two dips that we have labeled as λ_{bare} and λ_{PDMS}. When temperature is raised the refractive index of the water solution as well as the PDMS decreases, the TOC of these materials is negative. Both resonance dips shift toward shorter wavelengths but the displacement of the λ_{PDMS} is ten times larger than the λ_{bare}. When refractive index of external medium increases, keeping the temperature fixed to 20 °C, the plasmon conditions of the bare gold-coated fiber section changes and the resonance dip is red-shifted. The thickness of the PDMS layer is assumed to be larger than 1 mm so the external refractive index has not effect on the plasmon conditions in the polymerized fiber section. The effect of refractive index change in the transmitted spectra of the dual-signal SPR sensor is shown in Fig. 7(b). These theoretical curves predict that it is possible to measure the refractive index and temperature simultaneously using a dual-channel SPR-based optical fiber sensor. The refractive index of the SMF core and cladding as well as the water and PDMS were calculated using the Sellmeier coefficients reported in [54,55]. The theoretical model only considers meridional rays whose incident angle is larger than the critical angle in a multimode fiber. This and other assumptions are responsible of the differences in the wavelength and width of the resonant dip (λ_{bare}) in the theoretical spectra of Fig. 7(a) and (b) respect to the experimental transmission spectra of Figs. 3 and 4.

The MM-SM-MM structured fiber with a SMF length of 5 mm and coated with two diametrically opposed gold layers was selected since the resonance dip is relatively symmetric and narrow. Additionally, the device has a sensitive section long enough to facilitate the fabrication process and at the same time it can be considered as a compact sensor. The process that was used to fabricate the sensor can be described briefly as follows: the PDMS polymer was mixed with the curing agency and this mixture was allowed to stand until all air bubbles got out from it. Meanwhile, an acrylic piece was put over a Peltier plate and the gold-coated fiber was suspended over, in such way that a half section of the SMF is set one millimeter above the acrylic. Finally the PDMS was poured over the acrylic slice covering the half length of the gold-coated fiber section see Fig. 6(a). Due to surface tension the PDMS did not spill down from the acrylic. Finally, PDMS was cured by heating the sample at 80 °C for 6 h and this process produced that the half section of the gold-coated SMF was embedded in a PDMS film and this device was ready for simultaneous monitoring the RI and the temperature. During the PDMS coating and curing process the fiber transmission was monitored. At the moment that polymer was poured over the fiber a resonance dip appeared in the transmitted spectrum around 900 nm. After curing a small displacement of the resonance dip was observed, then the device was removed from the mount. In Fig. 6(b) a representation of the device fabricated is show, the rectangular

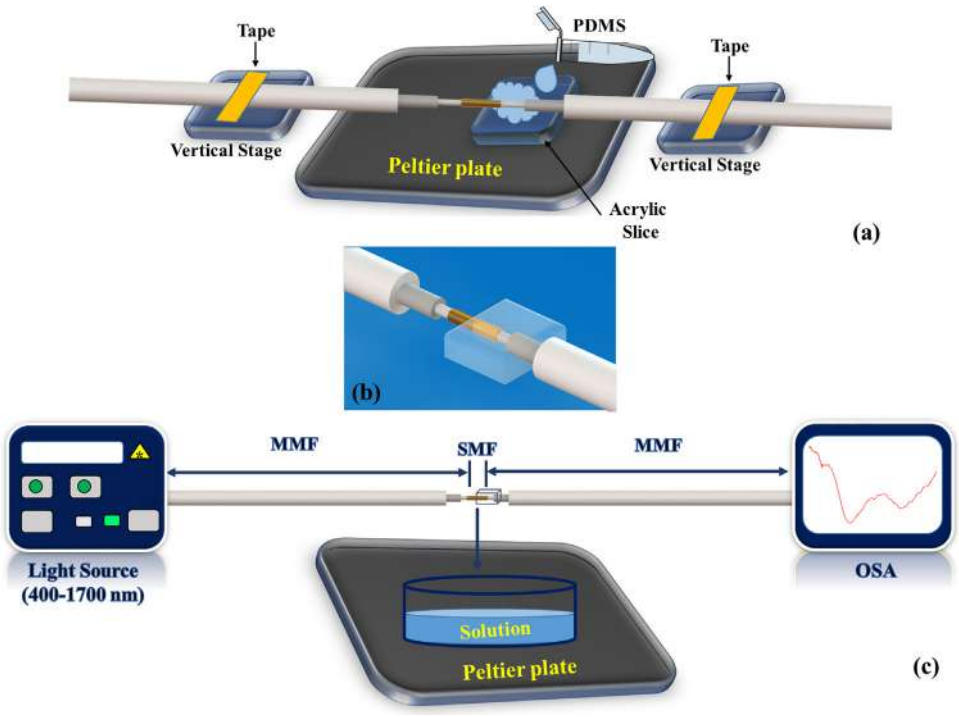

Fig. 6. Representation of: (a) the fabrication process of the sensor, (b) Dual-channel SPR optical fiber sensor proposed and (c) Experimental set-up to characterize the response of the sensor to refractive index and temperature variations.

shape of the polymer layer of our sensor is easier to manipulate but a number of different PDMS shapes can be obtained, according to the requirements of the application. It is important to mention that this sensor is highly sensitive to bending so the device have to keep fixed during the test.

4. Simultaneous measurement of refractive index and temperature: results and discussion

Once the fabrication process was completed, the sensitivity to temperature and RI of the devices were characterized using a transmission set-up similar to that represented in Fig. 6(b). Firstly, the device was put over a Peltier plate and then heated from 20 to 60 °C in order to determine the device response to temperature changes. It is well-known that the refractive index of the PDMS decreases (increases) as the temperature increases (decrease), so when the sensor was heated the refractive index of the PDMS layer, in close contact with the gold thin film, decreases. The experimental transmitted spectra of the fiber sensor at 25, 35, 45 and 55 °C are shown in Fig. 8(a). It is important to mention that the spectra exhibit a single dip at a wavelength (λ_{PDMS}) since the bare gold-coated fiber section is surrounding by air. As the temperature increases, the PDMS refractive index decreases and this produce a blue-shift in the wavelength of the resonance dip. The characteristic curve of temperature vs wavelength resonance dip shift ($\Delta\lambda_{PDMS}$) is shown in Fig. 8(b). The temperature sensitivity of the SPR-based optical fiber when is covered with PDMS is −2.861 nm/°C.

When the device was immersed in water-glycerol solutions a second dip λ_{bare}, at shorter wavelength than that of λ_{PMDS}, appeared. The wavelength position of both dips is dependent on the refractive index and temperature of the solutions. The transmitted spectra obtained when the fiber is immersed in solutions with refractive index of 1.346 (black line), 1.365 (red line) and 1.388 (blue line) at 20 °C are shown in Fig. 9(a). The refractive index of the water-glycerol solutions was measured with an Abbe refractometer. As the refractive index of the solution increases, λ_{bare} shifts toward longer wavelengths, reducing the separation between dips and affecting seriously the shape of the dips, which become less defined as in the case the solution with a RI of 1.388. This RI can be stablished as the superior limit of the dynamic range. The initial separation between the λ_{bare} and λ_{PDMS} can be increased by coating the bare gold-coated fiber section with a proper metal or dielectric layer [24,26,27,30–34,56,57]. The shift of the resonance dips due to refractive index changes are shown in Fig. 9(b), it is important to notice that the polymerized fiber section is insensitive to the refractive index change. The sensitivity of the bare and polymerized gold-coated fiber section to refractive index changes were 2323.4 and 0 nm/RIU, respectively.

While the fiber sensor was immersed in these solutions the temperature was increased from 20 to 60 °C. The transmitted spectra when the fiber sensor was immersed in 90%water-10%glycerol solution, with a refractive index of 1.346, while the temperature was 25 (black line), 35 (red line), 45 (blue line) and 55 °C (pink line) are shown in Fig. 10(a). Both resonance dips exhibited a blue-shift but the displacement of λ_{PMDS} is ten times larger than that of the λ_{bare}. The response of the device to temperature changes is summarized in the graphs of Fig. 10(b). The temperature sensitivity of the first and second peak, for a 90%water/10%glycerol solution, were −0.28 and −2.85 nm/°C, respectively. The temperature sensitivity of the dual-signal SPR sensor calculated is very similar to that obtained in the previous section when the device was tested in ambient air.

Changes in temperature (ΔT) and refractive index (Δn) produce changes in wavelength of the resonance dips ($\Delta\lambda_{bare}$ and $\Delta\lambda_{PDMS}$), this relation can be mathematically expressed by the following set of equations:

$$\begin{bmatrix} \Delta\lambda_{bare} \\ \Delta\lambda_{PDMS} \end{bmatrix} = \begin{bmatrix} -0.280 & 2323.4 \\ -2.85 & 0 \end{bmatrix} \begin{bmatrix} \Delta T \\ \Delta n \end{bmatrix} \quad (1)$$

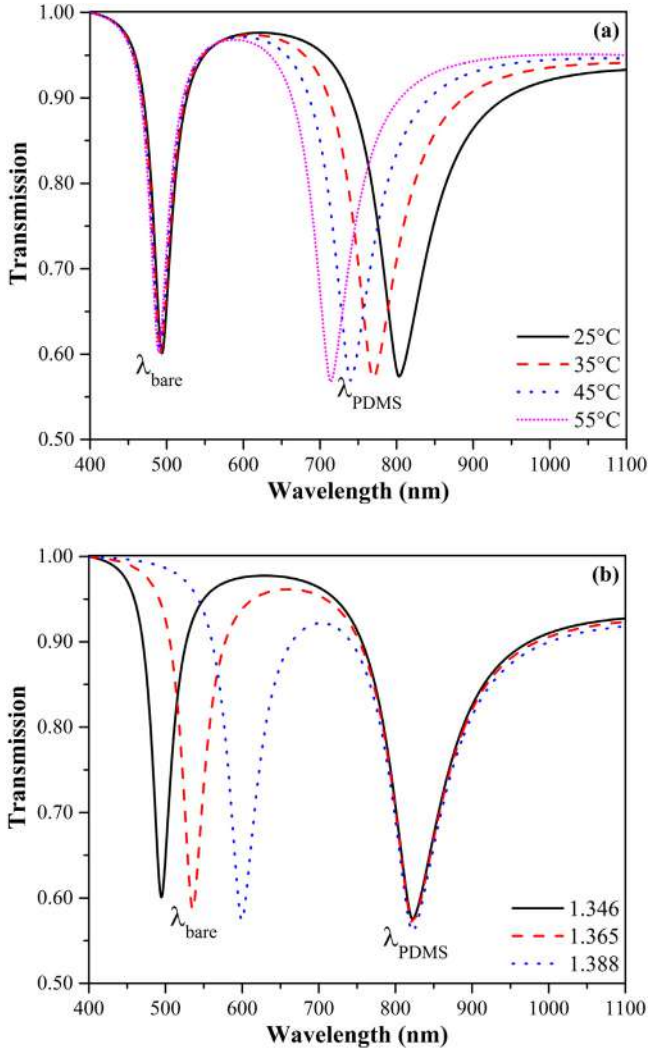

Fig. 7. (a) Theoretical transmission spectra of the sensor when it is immersed in solution with refractive index of 1.346 at four temperatures: 25 (black line), 35 (red line), 45 (blue line) and 55 °C (pink line) and (b) Immersed in solutions with refractive index of 1.346 (black line), 1.365 (red line) and 1.388 (blue line); at a fixed temperature of 20 °C. (For interpretation of the references to colour in this figure legend, the reader is referred to the web version of this article.)

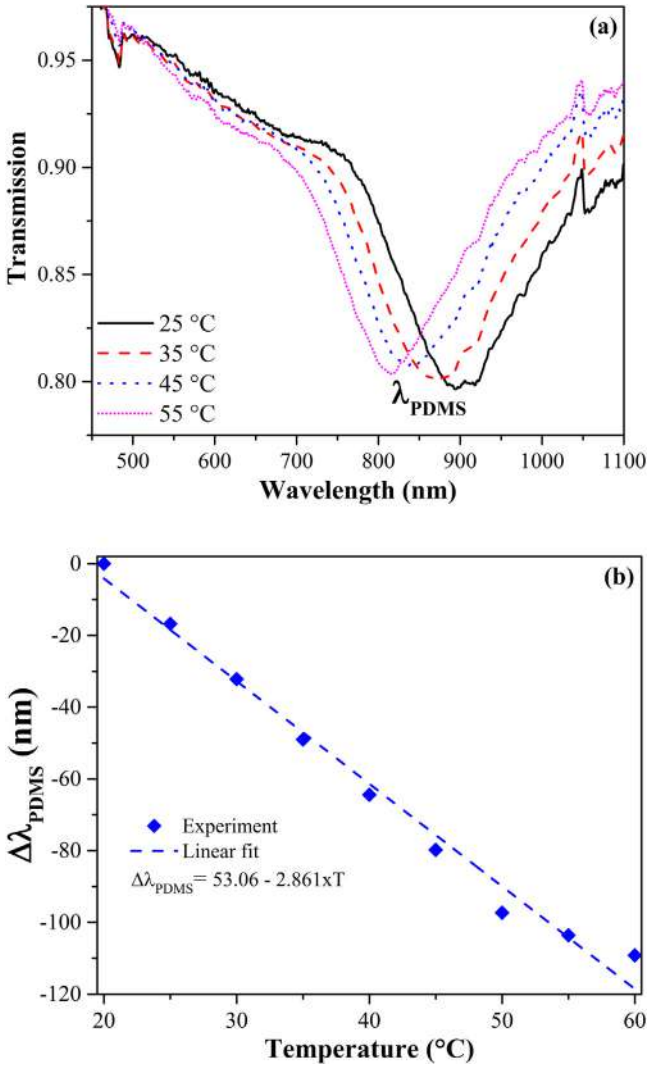

Fig. 8. (a) Experimental transmission spectra of the sensor at four temperatures: 25 (black line), 35 (red line), 45 (blue line) and 55 °C (pink line). (b) Experimental curve of the sensor response characterization to temperature changes.

Finally, the sensing matrix can be then expressed as:

$$\begin{bmatrix} \Delta T \\ \Delta n \end{bmatrix} = \frac{1}{(2.85)(2323.4)} \begin{bmatrix} 0 & -2323.4 \\ 2.85 & -0.280 \end{bmatrix} \begin{bmatrix} \Delta\lambda_{bare} \\ \Delta\lambda_{PDMS} \end{bmatrix} \quad (2)$$

where the units of $\Delta\lambda_{bare}$ and $\Delta\lambda_{PDMS}$ are in nm, while ΔT is in °C and Δn in RIU. Temperature change ΔT can be determined by measuring $\Delta\lambda_{PDMS}$, so the total refractive index change can be now described by

$$\Delta n = 4.3 \times 10^{-4} \times \Delta\lambda_{bare} + 1.2 \times 10^{-4} \times \Delta T \quad (3)$$

As was discussed previously the shift of λ_{bare} is resulted from the combined effect of the refractive index of the substance under test and the substance refractive index change with temperature. The second contribution is responsible for the uncertainty on the measurement of Δn. The second term of equation 3 effectively compensate the thermal perturbation on the substance refractive index. As can be seen the coefficient of the second term is very close to that of the first term, in this case, ΔT is larger than $\Delta\lambda_{bare}$, so the contribution of the second term could be larger than that the first term, for ΔT values as small as 5 °C. Therefore, in a SPR biosensor the measurement or compensation of the thermal perturbations is mandatory.

It is worth to notice that the experiments were carried out with a hot plate, isolated from environmental ambient temperature, the minimum temperature change of this equipment was 1 grade centigrade. Our device was able to measure such change since the sensitivity was approximately 2.9 nm/°C. We can speculate that temperature detection limit, assuming the OSA resolution of 0.1 nm, is around 0.05 °C. The same argument could be applied to the refractive index detection limit of our device, we calculate a value around 5×10^{-5} RIU. Considering this refractive index detection limit, we estimate that if fiber sensor is immersed in water the minimum temperature change that can produce a detectable refractive index change is 0.5 °C. It should be mentioned that the PDMS polymer is a hydrophobic material which means that being in contact with water solution does not affects its properties [58], nevertheless; an experiment was accomplished where the device was immersed in water during 12 h and the spectrum was recorded each hour. No change in the wavelength resonance dip was observed during this experiment.

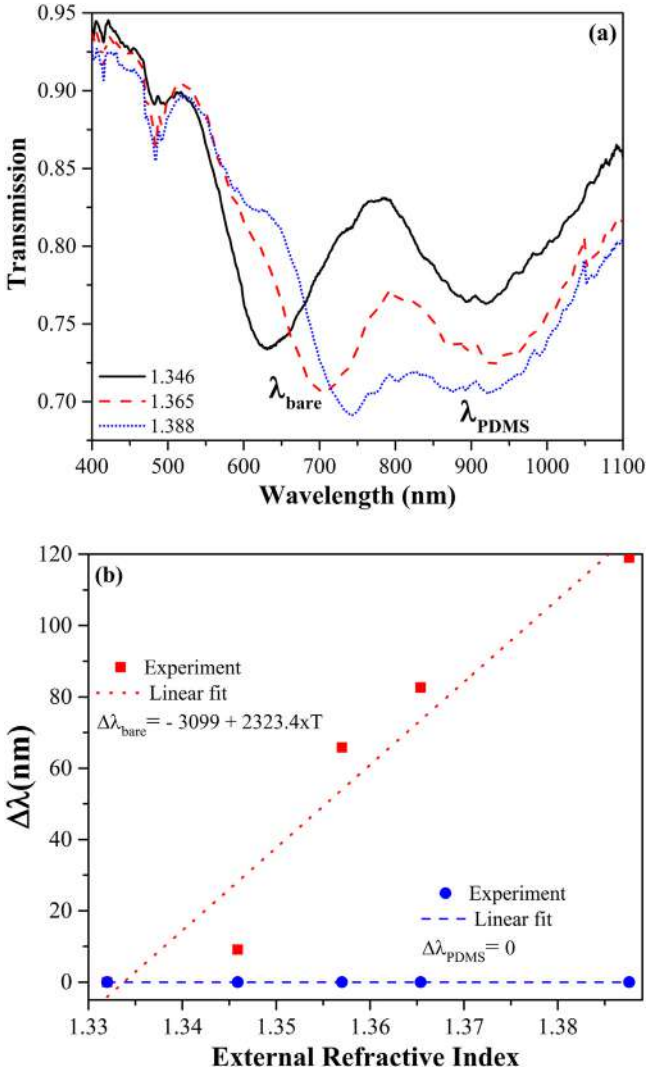

Fig. 9. (a) Experimental transmission spectra of the fiber sensor immersed at three different water-glycerol solutions: 1.346 (black line), 1.365 (red line) and 1.388 (blue line); at a fixed temperature of 20 °C. (b) Experimental characterization curve of the sensor response to refractive index changes.

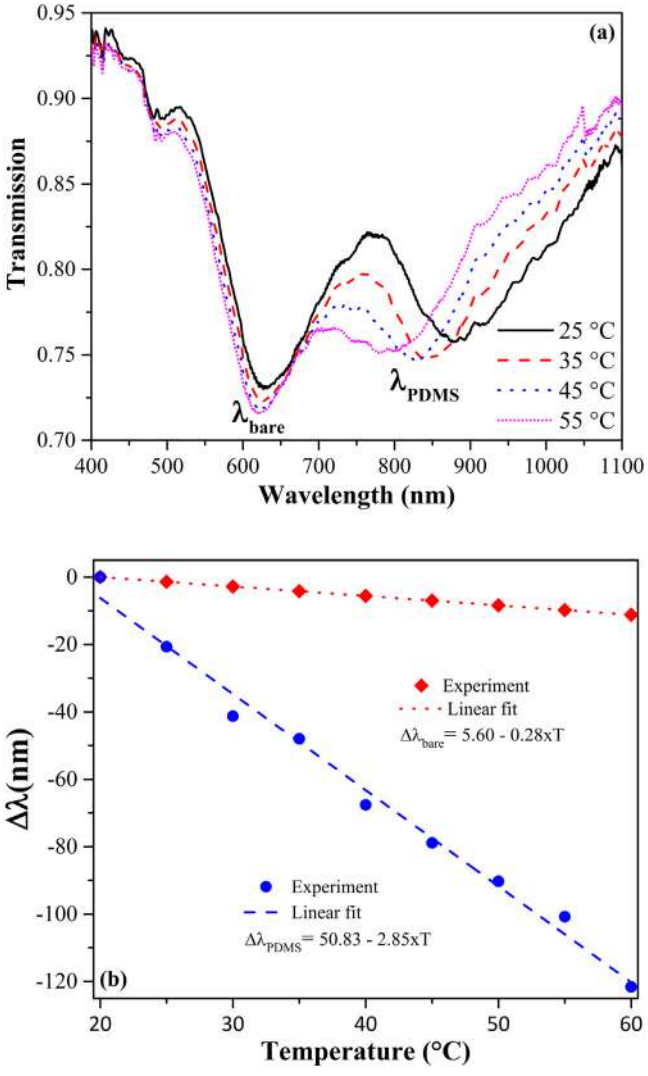

Fig. 10. (a) Experimental transmission spectra of the fiber sensor immersed in 90%water-10%glycerol at four temperatures 25 (black line), 35 (red line), 45 (blue line) and 55 °C (pink line). (b) Experimental characterization curve of the sensor response to temperature changes.

5. Conclusions

A dual-channel SPR-based optical fiber sensor for simultaneous monitoring temperature and refractive index of a liquid sample is proposed and demonstrated, for the first time to our knowledge. The sensor consists of a MM-SM-MM structured fiber with a single-mode fiber section of 5 mm length coated with a double-sided gold layer of 30 nm. Half of the gold-coated SMF section was covered with a high TOC polymer (PDMS). The polymerized fiber section give rise to a plasmon resonance dip at a wavelength (λ_{PDMS}) around 900 nm. When fiber sensor is immersed in a liquid sample a second resonance dip appears at a wavelength (λ_{bare}) determined by the refractive index of the sample. Changes in the liquid temperature produce a wavelength shift of both dips, while refractive index changes only affect the wavelength of the λ_{bare} dip. The sensor proposed is compact, easy to fabricate and manipulate, the sensitivity to temperature and refractive index is high. This device can be integrated in sensing networks or in a microfluidic chip for biosensing applications.

Acknowledgments

The authors are grateful to the Consejo Nacional de Ciencia y Tecnología (CONACyT – México) for financial support. The authors are grateful to the Dirección de Investigación, the mechanical and optical workshop from Centro de Investigaciones en Óptica A. C. for their support and assistance in the fabrication of some samples. J.S. Velázquez-González acknowledges CONACyT for their support through a Ph.D. scholarship and BEIFI (IPN-SIP) for their scholarship. I. Hernández-Romano acknowledges the funding through the project: "Cátedras CONACYT 2015". This work was funded by CONACYT under the *CIENCIA BASICA* project No. 257046.

References

[1] Jingyi Lou, Yipei Wang, Limin Tong, Microfiber optical sensors: a review, Sensors 14 (2014) 5823–5844.
[2] Xu-dong Wang, Otto S. Wolfbeis, Fiber-optic chemical sensors and biosensors (2013–2015), Anal. Chem. 88 (2016) 203–227.
[3] Armando Ricciardi, Alessio Crescitelli, Patrizio Vaiano, Giuseppe Quero, Marco Consales, Marco Pisco, Emanuela Esposito, Andrea Cusano, Lab-on-fiber technology: a new vision for chemical and biological sensing, Analyst 140 (2015) 8068–8079.

[4] Matías Calcerrada, Carmen García-Ruiz, Miguel González-Herráez, Chemical and biochemical sensing applications of microstructured optical fiber-based systems, Laser Photonics Rev. 9 (2015) 604–627.
[5] Christophe Caucheteur, Tuan Guo, Jacques Albert, Review of plasmonic fiber optic biochemical sensors: improving the limit of detection, Anal. Bioanal. Chem. 407 (2015) 3883–3897.
[6] Robert Blue and Deepak Uttamchandani, Recent advances in optical fiber devices for microfluidics integration, J. Biophotonics 9 (2016) 13–25.
[7] A. Ping Zhang, Li-Yang Shao, Jin-Fei Ding, Sailing He, Sandwiched long-period gratings for simultaneous measurement of refractive index and temperature, IEEE Photonics Technol. Lett. 17 (2005) 2397–2399.
[8] Hae Young Choi, Gopinath Mudhana, Kwan Seob Park, Un-Chul Paek, Byeong Ha, Cross-talk free and ultra-compact fiber optic sensor for simultaneous measurement of temperature and refractive index, Opt. Express 18 (2009) 141–149.
[9] Huanhuan Liu, Fufei Pang, Hairui Guo, Wenxin Cao, Yunqi Liu, Na Chen, Zhenyi Chen, Tingyun Wang, In-series double cladding fibers for simultaneous refractive index and temperature measurement, Opt. Express 18 (2010) 13072–13082.
[10] Allan C.L. Wong, W.H. Chung, Hwa-Yaw Tam, Chao Lu, Single tilted Bragg reflector fiber laser for simultaneous sensing of refractive index and temperature, Opt. Express 19 (2011) 409–414.
[11] Young Ho Kim, Seong Jun Park, Sie-Wook Jeon, Seongmin Ju, Chang-Soo Park, Won- Taek Han, Byeong Ha Lee, Thermo-optic coefficient measurement of liquids based on simultaneous temperature and refractive index sensing capability of a two-mode fiber interferometric probe, Opt. Express 20 (2012) 23744–23754.
[12] Ruchi Garg, Saurabh Mani Tripathi, Krishna Thyagarajan, Wojtek J. Bock, Long period fiber grating based temperature-compensated high performance sensor for bio-chemical sensing applications, Sens. Actuators B 176 (2013) 1121–1127.
[13] Carlos Gouveia, Giancarlo Chesinic Cristiano, M.B. Cordeiro, J.M. Baptista, Pedro A.S. Jorge, Simultaneous measurement of refractive index and temperature using multimode interference inside a high birefringence fiber loop mirror, Sens. Actuators B 177 (2013) 717–723.
[14] Qizhen Sun, Haipeng Luo, Hongbo Luo, Macheng Lai, Deming Liu, Lin Zhang, Multimode microfiber interferometer for dual parameters sensing assisted by Fresnel reflection, Opt. Express 23 (2015) 12777–12783.
[15] Guolu Yin, Yiping Wang, Changrui Liao, Bing Sun, Yingjie Liu, Shen Liu, Qiao Wang, Kaiming Yang, Jian Tang, Xiaoyong Zhong, Simultaneous refractive index and temperature measurement with LPFG and liquid filled PCF, IEEE Photonics Technol. Lett. 27 (2015) 375–378.
[16] C.R. Liao, Ying Wang, D.N. Wang, M.W. Yang, Fiber in-line Mach?Zehnder interferometer embedded in FBG for simultaneous refractive index and temperature measurement, IEEE Photonics Technol. Lett. 22 (2010) 1686–1689.
[17] Woong Jung Il, Bryan Park, J. Provine, Roger T. Howe, Olav Solgaard, Highly sensitive monolithic silicon photonic crystal fiber tip sensor for simultaneous measurement of refractive index and temperature, IEEE Photonics Technol. Lett. 29 (2011) 1367–1369.
[18] Simon Pevec, Denis Donlagic, High resolution, all-fiber, micro-machined sensor for simultaneous measurement of refractive index and temperature, Opt. Express 22 (2014) 16241–16253.
[19] Jian Wang, Shengli Wu, Wenyi Ren, Simultaneous measurement of refractive index and temperature using an epoxy resin-based interferometer, App. Opt. 53 (2014) 7825–7830.
[20] Min Li, Yi Liu, Xiuli Zhao, Shiliang Qu, Yan Li, Miniature □-shaped polymer fiber tip for simultaneous measurement of the liquid refractive index and temperature with high sensitivities, J. Opt. 17 (2015) 105701.
[21] Chun-Fan Chan, Chengkun Chen, Amir Jafari, Albane Laronche, Douglas J. Thomson, Jacques Albert, Optical fiber refractometer using narrowband cladding-mode resonance shifts, Appl. Opt. 46 (2007) 1142–1149.
[22] Xiaowei Guo, Surface plasmon resonance based biosensor technique: a review, J. Biophotonics 5 (2012) 483–501.
[23] Yun Liu, Qiang Liu, Shimeng Chen, Fang Cheng, Hanqi Wang, Wei Peng, Surface plasmon resonance biosensor based on smart phone platforms, Sci. Rep. 5 (2015) 12864.
[24] Yun Liu, Shimeng Chen, Qiang Liu, Jean-François Masson, Wei Peng, Compact multi-channel surface plasmon resonance sensor for real-time multi-analyte biosensing, Opt. Express 23 (2015) 20540–20548.
[25] Iulia Arghir, Dragana Spasic, Bert E. Verlinden, Filip Delport, Jeroen Lammertyn, Improved surface plasmon resonance biosensing using silanized optical fibers, Sens. Actuators B: Chem. 216 (2015) 518–526.
[26] Roli Verma, Banshi D. Gupta, A novel approach for simultaneous sensing of urea and glucose by SPR based optical fiber multianalyte sensor, Analyst 139 (2014) 1449–1455.
[27] A. Francois, J. Boehm, S.Y. Oh, T. Kok, T.M. Monro, Collection mode surface plasmon fibre sensors: a new biosensing platform, Biosens. Bioelectron. 26 (2011) 3154–3159.
[28] Jirí Homola, Hana Vaisocherová, Jakub Dostálek, Marek Piliarik, Multi-analyte surface plasmon resonance biosensing, Methods 37 (2005) 26–36.
[29] Jakub Dostálek, Hana Vaisocherová, Jirí Homola, Multichannel surface plasmon resonance biosensor with wavelength division multiplexing, Sens. Actuators B: Chem. 108 (2005) 758–764.
[30] Wei Peng, Soame Banerji, Yoon-Chang Kim, Karl S. Booksh, Investigation of dual-channel fiber-optic surface plasmon resonance sensing for biological applications, Opt. Lett. 30 (2005) 2988–2990.
[31] Zhiyi Zhang, Ping Zhao, Fengguo Sun, Gaozhi Xiao, Yaming Wu, Self-Referencing in optical-fiber surface plasmon resonance sensors, IEEE Photonics Technol. Lett. 19 (2007) 1958–1960.
[32] Yinquan Yuan, Lina Wang, Jun Huang, Theoretical investigation for two cascaded SPR fiber optic sensors, Sens Actuators B: Chem. 161 (2012) 269–273.
[33] Shimeng Chen, Yun Liu, Qiang Liu, Wei Peng, Temperature-Compensating fiber-optic surface plasmon resonance biosensor, IEEE Photonics Technol. Lett. 28 (2016) 312–315.
[34] Sijun Weng, Li Pei, Chao Liu, Jianshuai Wang, Jing Li, Tigang Ning, Double-side polished fiber SPR sensor for simultaneous temperature and refractive index measurement, IEEE Photonics Technol. Lett. 28 (2016) 1916–1919.
[35] A.W. Snyder, J.D. Love, Optical Waveguide Theory, Chapman and Hall, London New York, 1983.
[36] Jacques Bures, Guided Optics: Optical Fibers and All-Fiber Components, Wiley-VCH, Weinheim Germany, 2009.
[37] Joel Villatoro, David Monzón-Hernández, Low-Cost optical fiber refractive-index sensor based on core diameter mismatch, J. Lightw. Technol. 24 (2006) 1409–1413.
[38] Mitsuhiro Iga, Atsushi Seki, Kazuhiro Watanabe, Hetero-core structured fiber optic surface plasmon resonance sensor with silver film, Sens. Actuators B Chem. 101 (2004) 368–372.
[39] Mitsuhiro Iga, Atsushi Seki, Kazuhiro Watanabe, Gold thickness dependence of SPR-based hetero-core structured optical fiber sensor, Sens. Actuators B Chem. 106 (2005) 363–368.
[40] Jiri Homola, Sinclair S. Yee, Gunter Gauglitz, Surface plasmon resonance sensors: review, Sens. Actuators B 54 (1999) 3–5.
[41] David Monzón-Hernández, Joel Villatoro, High-resolution refractive index sensing by means of a multiple-peak surface plasmon resonance optical fiber sensor, Sens. Actuators B 115 (2006) 227–231.
[42] Natalia Díaz Herrera, Óscar Esteban, María-Cruz Navarrete, Agustín González-Cano, Elena Benito-Peña, Guillermo Orellana, Improved performance of SPR sensors by a chemical etching of tapered optical fibers, Opt. Laser Eng. 49 (2011) 1065–1068.
[43] Y. Shevchenko, C. Chen, M.A. Dakka, J. Albert, Polarization-selective grating excitation of plasmons in cylindrical optical fibers, Opt. Lett. 35 (2010) 637–639.
[44] María-Cruz Navarrete, Natalia Díaz-Herrera, Agustín González-Cano, Óscar Esteban, A polarization-independent SPR fiber sensor, Plasmonics 5 (2010) 7–12.
[45] Hitoshi Suzukia, Mitsunori Sugimoto, Yoshikazu Matsui, Jun Kondoh, Effects of gold film thickness on spectrum profile and sensitivity of a multimode-optical-fiber SPR sensor, Sen. Actuators B: Chem. 132 (2008) 26–33.
[46] Torsten Wieduwilt, Konstantin Kirsch, Jan Dellith, Reinhardt Willsch, Hartmut Bartelt, Optical fiber micro-taper with circular symmetric gold coating for sensor applications based on surface plasmon resonance, Plasmonics 8 (2013) 545–554.
[47] Agustín González-Cano, Francisco-Javier Bueno, Óscar Esteban, Natalia Díaz-Herrera, María-Cruz Navarrete, Multiple surface-plasmon resonance in uniform-waist tapered optical fibers with an asymmetric double-layer deposition, Appl. Opt. 44 (2005) 519–526.
[48] Dingyi Feng, Wenjun Zhou, Xueguang Qiao, Jacques Albert, High resolution fiber optic surface plasmon resonance sensors with single-sided gold coatings, Opt. Express 24 (2016) 16456–16464.
[49] Antonio Díez, Miguel V. Andrés, José L. Cruz, Hybrid surface plasma modes in circular metal-coated tapered fibers, J. Opt. Soc. Am. A 16 (1999) 2979–2982.
[50] Donato Luna-Moreno, David Monzón-Hernández, Effect of the Pd–Au thin film thickness uniformity on the performance of an optical fiber hydrogen sensor, Appl. Surf. Sci. 253 (2007) 8615–8619.
[51] Li-Yang Shao, Yanina Shevchenko, Jacques Albert, Intrinsic temperature sensitivity of tilted fiber Bragg grating based surface plasmon resonance sensors, Opt. Express 18 (2010) 11464–11471.
[52] Yong Zhao, Ze-Qun Deng, Hai-Feng Hu, Fiber-optic SPR sensor for temperature measurement, IEEE Trans. Instrum. Meas. 64 (2015) 3099–30104.
[54] Y. Yuan, L. Ding, Z. Guo, Numerical investigation for SPR-based optical fiber sensor, Sens. Actuators B Chem. 157 (2011) 240–245.
[55] F. Schneider, J. Draheim, R. Kamberger, Ulrike Wallrabe, Process and material properties of polydimethylsiloxane (PDMS) for Optical MEMS, Sens. Actuators A: Phys. 151 (2009) 95–99.
[56] Zhihai Liu, Yong Wei, Yu Zhang, Yushan Wang, Enming Zhao, Yaxun Zhang, Jun Yang, Chunyu Liu, Libo Yuan, A multi-channel fiber SPR sensor based on TDM technology, Sens. Actuators B 226 (2016) 326–331.
[57] Zhihai Liu, Yong Wei, Yu Zhang, Chunlan Liu, Yaxun Zhang, Enming Zhao, Jun Yang, Libo Yuan, Compact distributed fiber SPR sensor based on TDM and WDM technology, Opt. Express 23 (2015) 24004–24012.
[58] Joseph C. Spagnola, Bo Gong, Gregory N. Parsons, Surface texture and wetting stability of polydimethylsiloxane coated with aluminum oxide at low temperature by atomic layer deposition, J. Vac. science Technol. A 28 (2013) 1330–1337.

Biographies

J. S. Velázquez-González received a B.Eng. degree in Communications and Electronic and his M.Sc. degree in Electronic Engineering at Instituto Politécnico Nacional (IPN – ESIME Zacatenco and SEPI-ESIME Zacatenco) in 2008 and 2011, respectively. Since October 2015 he is academic visitor in the optical sensors and microdevices group at The Centro de Investigaciones en Optica A. C. Now he is pursuing a Ph.D. in Optical Fiber Sensors at Centro de Investigación e Innovación Tecnológica (CIITEC-IPN). His research interest range from optical fiber devices and sensors to light-tissue interaction and image processing.

D. Monzón-Hernández obtained the Electron. Engineering, MSc and Ph. D degree from the Universidad of Guanajuato. Since 2002 he is with the Centro de Investigaciones en Óptica A. C. He is part of the optical sensors and microdevices group. His research activity is focused on the development of advanced optical sensing techniques based on novel optical fiber devices. These include optical microfiber Mach-Zehnder interferometer, extrinsic all optical fiber Fabry-Perot interferometers or metal-coated fiber tapers. The aim is to develop integrated low cost optical sensors for monitoring the presence of hazardous contaminants in water. The present research activity of Dr. Monzón is focused on the development of multi-parameter platform sensing and photonic devices based on surface plasmon resonance integrated in microfluidics circuits.

D. Moreno-Hernández received his PhD degree in Optics in 2000 from the Centre for Research in Optics (CIO) in Mexico. Prior to joining as a researcher at CIO in 2003, he was a postdoctoral scholar in the Mechanical Engineering Department at the Florida State University. His research interest is temperature and velocity measurements in fluid flows, digital holography and data analysis.

F. Martínez-Piñón received a B.Eng. degree in communications and electronics at IPN in 1981, an MSc in electronics in 1984 at Southampton University and a PhD in optical fiber technology at the Optoelectronics Research Centre also from Southampton University in 1988. He was a researcher of the Electrical Research Institute and designed optical fiber networks for Iusacell and Unefon in Mexico. He was director of the Information Technologies Cooperation Centre between Mexico and South Korea. He is a senior research fellow at CIITEC-IPN since 2005. His research interests are the development of fiber devices for telecommunications and sensor applications.

I. Hernández-Romano received the B.Sc. degree in physics from the Facultad de Ciencias Fisico Matematicas, BUAP, and the M.Sc. and Ph.D. degree in optics from the National Institute for Astrophysics, Optics and Electronics, Puebla, Mexico, in 2007 and 2011, respectively. He is currently a CONACYT Research Fellow-Electronics Department, Sede Palo Blanco, University of Guanajuato. His current research interests include optical fiber sensor and their applications.